

Hybrid Free-Space Optical and Radio-Frequency Communications: Outage Analysis

Nick Letzepis*, Khoa D. Nguyen*, Albert Guillén i Fàbregas[†], and William G. Cowley*

*Institute for Telecommunications Research, University of South Australia, Mawson Lakes SA 5095

[†]University of Cambridge, Department of Engineering, Cambridge CB2 1PZ UK

nick.letzepis@unisa.edu.au; dangkhoa.nguyen@unisa.edu.au;

guillen@ieee.org; bill.cowley@unisa.edu.au.

Abstract—We study hybrid free-space optical (FSO) and radio-frequency (RF) communications, whereby information is conveyed simultaneously using both optical and RF carriers. We consider the case where both carriers experience scintillation, which is a slow fading process compared to typical data rates. A parallel block-fading channel model is proposed, that incorporates differences in signalling rates, power scaling and scintillation models between the two carriers. Under this framework, we study the outage probability in the large signal-to-noise ratio (SNR) regime. First we consider the case when only the receiver has perfect channel state information (CSIR case) and obtain the SNR exponent for general scintillation distributions. Then we consider the case when perfect CSI is known at both the receiver and transmitter, and derive the optimal power allocation strategy that minimises the outage probability subject to peak and average power constraints. The optimal solution involves non-convex optimisation, which is intractable in practical systems. We therefore propose a suboptimal algorithm that achieves the same diversity as the optimal one and provides significant power savings (on the order of tens of dBs) over uniform allocation.

I. INTRODUCTION

Free-space optical (FSO) communication has the potential to provide fiber-like data rates with the advantages of quick deployment times, high security and no frequency regulations. Unfortunately such links are highly susceptible to atmospheric effects. *Scintillation* induced by atmospheric turbulence causes random fluctuations in the received irradiance of the optical laser beam [1]. Numerous studies have shown that performance degradation caused by scintillation can be significantly reduced through the use of multiple-lasers and multiple-apertures, creating the well-known multiple-input multiple-output (MIMO) channel (see e.g. [2]–[5]). However, it is the large attenuating effects of cloud and fog that pose the most formidable challenge. Extreme low-visibility fog can cause signal attenuation on the order of hundreds of decibels per kilometre [6]. One method to improve the reliability in these circumstances is to introduce a radio frequency (RF) link to create a *hybrid FSO/RF* communication system [6]–[8]. When the FSO link is blocked by cloud or fog, the RF link maintains reliable communications, albeit at a reduced data rate. Typically a millimetre wavelength carrier is selected for the RF link to achieve data rates comparable to that of the

FSO link. At these wavelengths, the RF link is also subject to atmospheric effects, including rain and scintillation [9], [10], but is less affected by fog. The two channels are therefore complementary: the FSO signal is severely attenuated by fog, whereas the RF signal is not; and the RF signal is severely attenuated by rain, whereas the FSO is not. Both, however, are affected by scintillation.

Lacking so far in the literature on hybrid FSO/RF channels is the development of a suitable channel model and its theoretical analysis to determine the fundamental limits of communication. This is the central motivation for our paper. We propose a hybrid channel model based on the well known parallel channel [11], and take into account the differences in signalling rate, and the atmospheric fading effects present in both the FSO and RF links. These fading effects are slow compared to typical data rates, and as such, each channel is based on a *block-fading* channel model. First we examine the case when perfect CSI is known at the receiver only (CSIR case), then we consider the case when CSI is also known at the transmitter (CSIT case), and power allocation is employed to reduce the outage probability subject to power constraints. For the CSIR case we calculate the SNR exponents of the hybrid channels for general scintillation distributions in each of the channels. Then for the CSIT case, we derive the optimal power allocation algorithm subject to both peak and average power constraints. This optimal solution involves non-convex optimisation, which has prohibitive complexity in practical systems. We therefore propose a suboptimal solution and prove that it has the same SNR exponent as optimal power allocation.

The remainder of this paper is organised as follows. In Section II we present our channel model and assumptions. Section III presents our main results for the CSIR-only case while Section IV discusses power allocation and SNR exponents for the CSIT case. Section V draws final concluding remarks. Detailed proofs of our results can be found in [12].

II. CHANNEL MODEL AND ASSUMPTIONS

Consider a hybrid FSO communication system where a binary data sequence is binary encoded into parallel FSO and RF bit streams. The RF link modulates the encoded bits and up-converts the baseband signal to a millimetre wavelength RF carrier frequency. The FSO link employs intensity modulation and direct detection, i.e. information is modulated using only

This work has been supported by the Sir Ross and Sir Keith Smith Fund, Cisco Systems as well as the Australian Research Council under ARC grants RN0459498, DP0558861 and DP088160.

the irradiance of a laser beam. The RF and FSO signals are transmitted simultaneously through an atmospheric channel. The received RF signal is then downconverted to baseband and sent to the decoder. At the same time, the received irradiance is collected by an aperture, converted to an electrical signal via photodetection and sent to the decoder. The received signals are jointly decoded to recover the transmitted message.

We define a *hybrid channel symbol*, $(\mathbf{x}, \hat{x}) \in \mathcal{X}_{\text{fso}}^n \times \mathcal{X}_{\text{rf}}$, consisting of component FSO and RF symbols, which are transmitted in parallel with perfect synchronism and have the same symbol period T_s . The RF component symbol, denoted by \hat{x} , is drawn uniformly from a complex signal set $\mathcal{X}_{\text{rf}} \subset \mathbb{C}$ of size $|\mathcal{X}_{\text{rf}}| = M = 2^m$, with unit average energy, i.e. $\mathbb{E}[|\hat{x}|^2] = 1$. Since the FSO link employs a much higher carrier frequency than the RF link, we assume the FSO component consists of n symbols drawn uniformly from a constellation \mathcal{X}_{fso} representing a pulse type modulation scheme, i.e. it consists of n symbols, which are further composed of Q pulse intervals of duration T_p , where $T_s = nQT_p$. The signal set $\mathcal{X}_{\text{fso}} \subset (0, 1)^Q$ is a set of Q length binary vectors, where a binary 1 at index i indicates a pulse of duration T_p in time slot i . We assume each T_p second ‘on’ pulse is normalised to have unit energy and denote the average FSO symbol energy by $\gamma = \mathbb{E}[\sum_{i=1}^Q x_i]$. Let $q \triangleq \log_2(|\mathcal{X}_{\text{fso}}|)$, hence the total bits per hybrid channel symbol is $m + nq$ bits.

Both FSO and RF channels are affected by scintillation [1], [9], [10], which is a slow fading process compared to typical data rates. We therefore propose a parallel block-fading channel model, whereby the component channels are divided into a finite number of blocks of symbols, and each block experiences an i.i.d. fading realisation. The scintillation experienced by each component channel is also assumed to be independent.¹ Typically, the RF scintillation has a coherence time on the order of seconds [9], [10], whereas the FSO scintillation is much faster, having a coherence time on the order of tens of milliseconds [1]. We therefore decompose the FSO and RF components of the codeword into A and B blocks of K and L symbols respectively, where $A \geq B$.² Note that the total number of symbols in each FSO/RF component codeword is the same, i.e. $AK = BL$. We assume that the number of symbols in each block tends to infinity, but the ratio remains a fixed constant, i.e. $\lim_{K,L \rightarrow \infty} \frac{L}{K} = \frac{A}{B}$. We assume both FSO/RF component channels are modelled by independent additive white Gaussian noise (AWGN) channels.³ Hence we write the received FSO and RF signals as

$$\mathbf{y}_a[k] = p_a \rho h_a \mathbf{x}_a[k] + \mathbf{z}_a[k] \quad (1)$$

$$\hat{y}_b[l] = \sqrt{\hat{p}_b \hat{\rho} \gamma \hat{h}_b} \hat{x}_b[l] + \hat{z}_b[l], \quad (2)$$

¹This will be true over short time intervals, but over longer time scales meteorological variations will result in correlated channel fades.

²Given that the coherence time of the RF scintillation is on the order of seconds, the most realistic scenario is $B = 1$. However, for generality we will assume B is an arbitrary positive integer.

³Note that this assumption for the FSO channel may not be accurate under certain conditions [13].

for $l = 1, \dots, L$, $k = 1, \dots, K$, $a = 1, \dots, A$ and $b = 1, \dots, B$, where: $\mathbf{y}_a[k] \in \mathbb{R}^{nQ}$ and $\hat{y}_b[l] \in \mathbb{C}$ are the noisy received symbols for the FSO and RF channels respectively; $\mathbf{x}_a[k] \in \mathcal{X}_{\text{fso}}^n$ and $\hat{x}_b[l] \in \mathcal{X}_{\text{rf}}$ denote the transmitted symbols; $\mathbf{z}_a[k] \in \mathbb{R}^{nQ}$ is a i.i.d. vector of zero mean unit variance real Gaussian noise, and $z_b[l] \in \mathbb{C}$ is unit variance complex Gaussian noise ($\mathcal{CN}(0, 1)$); $h_a > 0$ and $\hat{h}_b > 0$ are independent random power fluctuations due to scintillation, each i.i.d. drawn from distributions f_H and $f_{\hat{H}}$ respectively, with normalisation $\mathbb{E}[h_a] = \mathbb{E}[\hat{h}_b] = 1$; p_a and \hat{p}_b denotes the power of block a and b for the FSO and RF channels respectively. The γ parameter in (2) ensures both FSO and RF symbols have the same energy. The parameters $0 < \rho, \hat{\rho} < 1$ in (1) and (2) model differences in the relative strengths of the two parallel channels, e.g. it reflects long-term fading effects due to rain, fog or cloud as well as other parameters such as aperture/antenna gains and propagation loss.⁴

In this paper, we consider two CSI scenarios: (1) CSI at receiver only, uniform power allocation is employed; (2) perfect CSI at both receiver and transmitter, transmit power allocation is employed to minimise outages subject to long-term and individual peak (or short-term) power constraints constraints, i.e.

$$\mathbb{E}[\langle \mathbf{p} \rangle] + \mathbb{E}[\langle \hat{\mathbf{p}} \rangle] \leq P_{\text{av}}, \quad (3)$$

$$\langle \mathbf{p} \rangle \leq P_{\text{peak}}^{\text{fso}} \quad \text{and} \quad \langle \hat{\mathbf{p}} \rangle \leq P_{\text{peak}}^{\text{rf}}, \quad (4)$$

where $\langle \mathbf{p} \rangle = \frac{1}{A} \sum_{a=1}^A p_a$ and $\langle \hat{\mathbf{p}} \rangle = \frac{1}{B} \sum_{b=1}^B \hat{p}_b$. Note that for the FSO channel (1), the amplitude of the received electrical signal is directly proportional to the transmitted optical power, due to the photodetection process [14]. As we shall see later, this scaling will significantly affect the design of power allocation strategies.

III. ASYMPTOTIC OUTAGE ANALYSIS: CSIR CASE

The *information outage probability* of the hybrid system is

$$P_{\text{out}}(P_{\text{av}}, R) \triangleq \Pr \left\{ I_{\text{tot}}(\mathbf{p}, \hat{\mathbf{p}}, \mathbf{h}, \hat{\mathbf{h}}) < R \right\}, \quad (5)$$

where $\mathbf{h} = (h_1, \dots, h_A)$, $\hat{\mathbf{h}} = (\hat{h}_1, \dots, \hat{h}_B)$, $\mathbf{p} = (p_1, \dots, p_A)$, $\hat{\mathbf{p}} = (\hat{p}_1, \dots, \hat{p}_B)$, R is the target rate of the system in bits per hybrid channel use and,

$$I_{\text{tot}}(\mathbf{p}, \hat{\mathbf{p}}, \mathbf{h}, \hat{\mathbf{h}}) = \frac{n}{A} \sum_{a=1}^A I_{\mathcal{X}_{\text{fso}}}^{\text{awgn}}(h_a^2 \rho^2 p_a^2) + \frac{1}{B} \sum_{b=1}^B I_{\mathcal{X}_{\text{rf}}}^{\text{awgn}}(\hat{h}_b \hat{\rho} \gamma \hat{p}_b), \quad (6)$$

is the instantaneous input-output mutual information [11], where $I_{\mathcal{X}}^{\text{awgn}}(u) \in (0, \log_2 |\mathcal{X}|)$ denotes the input-output mutual information of the AWGN channel with input constellation \mathcal{X} and SNR u .⁵

⁴Although in practise ρ and $\hat{\rho}$ are randomly varying with time (and are also most likely correlated random variables), we assume they remain unchanged over many codeword time intervals and therefore are fixed constants.

⁵Note that the achievable rate (6) implicitly assumes joint encoding and decoding across FSO and RF channels.

Rather than assuming a specific fading distribution model, we instead assume it is characterised by each channel's single block transmission SNR exponent, defined as

$$d_{\text{fso}}^{(i)} \triangleq \lim_{u \rightarrow \infty} - \frac{\log \Pr\{I_{\text{fso}}^{\text{awgn}}(h^2 u^2) < R_{\text{fso}}\}}{(\log u)^i} \quad (7)$$

$$d_{\text{rf}}^{(j)} \triangleq \lim_{u \rightarrow \infty} - \frac{\log \Pr\{I_{\text{rf}}^{\text{awgn}}(\hat{h}u) < R_{\text{rf}}\}}{(\log u)^j}, \quad (8)$$

for given component channel rate constraints R_{fso} and R_{rf} , where $i, j \in \{1, 2\}$.⁶

Suppose that perfect CSI is known only at the receiver (CSIR case). The transmitter allocates power uniformly across all blocks, i.e. $p_1 = \dots = p_A = \hat{p}_1 = \dots = \hat{p}_B = p = P_{\text{av}}$. Then we have the following result.

Theorem 3.1: Define component $d_{\text{fso}}^{(i)}$ and $d_{\text{rf}}^{(j)}$ as in (7) and (8) respectively. Suppose $\rho, \hat{\rho} > 0$ and $i = j = k$. Then,

$$d^{(k)} \triangleq \lim_{P_{\text{av}} \rightarrow \infty} - \frac{\log P_{\text{out}}(P_{\text{av}}, R)}{\log P_{\text{av}}} = \inf_{\mathcal{K}(\delta, R_c)} \left\{ d_{\text{fso}}^{(k)} \kappa_1 + d_{\text{rf}}^{(k)} \kappa_2 \right\} \quad (9)$$

$$\mathcal{K}(\delta, R_c) \triangleq \left\{ \kappa_1, \kappa_2 \in \mathbb{Z} : \delta \frac{\kappa_1}{A} + (1 - \delta) \frac{\kappa_2}{B} > 1 - R_c, \right. \\ \left. 0 \leq \kappa_1 \leq A, 0 \leq \kappa_2 \leq B \right\}, \quad (10)$$

where $R_c \triangleq R/(m + nq)$ and $\delta \triangleq \frac{nq}{m+nq}$ is the ratio of FSO bits to total transmitted bits.

From Theorem 3.1, we see that the overall SNR exponent depends on R_c, δ, A, B and the individual SNR exponents d_{fso} and d_{rf} in a non-trivial way. However, for the most basic and interesting scenario, $A = B = 1$, the solution to (9) reduces to a simple intuitive form.

Corollary 3.1: Suppose $A = B = 1$. The solution to (9) is divided into two cases as follows.

1) If $\delta \leq \frac{1}{2}$, then

$$d^{(k)} = \begin{cases} d_{\text{fso}}^{(k)} + d_{\text{rf}}^{(k)} & 0 < R_c \leq \delta \\ d_{\text{rf}}^{(k)} & \delta < R_c \leq 1 - \delta \\ \min(d_{\text{fso}}^{(k)}, d_{\text{rf}}^{(k)}) & 1 - \delta < R_c < 1. \end{cases} \quad (11)$$

2) If $\delta \geq \frac{1}{2}$, then

$$d^{(k)} = \begin{cases} d_{\text{fso}}^{(k)} + d_{\text{rf}}^{(k)} & 0 < R_c \leq 1 - \delta \\ d_{\text{fso}}^{(k)} & 1 - \delta < R_c \leq \delta \\ \min(d_{\text{fso}}^{(k)}, d_{\text{rf}}^{(k)}) & \delta < R_c < 1. \end{cases} \quad (12)$$

In most practical systems, $\delta \geq \frac{1}{2}$, i.e. in a hybrid symbol period, the number of transmitted FSO bits will be greater than the number of RF transmitted bits. From (12), we see that the highest diversity is achieved if the binary code rate R_c is set to be less than $1 - \delta = m/(m + nq)$, i.e. the total information rate is less than the maximum information rate of the stand-alone RF channel. If $1 - \delta < R_c \leq \delta$, the exponent is the same as a single FSO link. For high binary code rates, $\delta < R_c < 1$, the asymptotic performance is dominated by the worst of the two exponents.

⁶SNR exponents for typical scintillation distributions can be found in [2].

Theorem 3.2: Define component channel SNR exponents $d_{\text{fso}}^{(i)}$ and $d_{\text{rf}}^{(j)}$ as in (7) and (8) respectively. Suppose $i > j$ then the SNR exponent is

$$d^{(i)} = d_{\text{fso}}^{(i)} \left(1 + \left\lfloor \frac{A}{\delta} (\delta - R_c) \right\rfloor \right) \quad 0 < R_c \leq \delta \quad (13)$$

$$d^{(j)} = d_{\text{rf}}^{(j)} \left(1 + \left\lfloor \frac{B}{1 - \delta} (1 - R_c) \right\rfloor \right) \quad \delta < R_c < 1. \quad (14)$$

Otherwise, if $i < j$ then the SNR exponent is

$$d^{(j)} = d_{\text{rf}}^{(j)} \left(1 + \left\lfloor \frac{B}{1 - \delta} (1 - \delta - R_c) \right\rfloor \right) \quad 0 < R_c \leq 1 - \delta. \quad (15)$$

$$d^{(i)} = d_{\text{fso}}^{(i)} \left(1 + \left\lfloor \frac{A}{\delta} (1 - R_c) \right\rfloor \right) \quad 1 - \delta < R_c < 1 \quad (16)$$

Theorem 3.2 shows how the overall performance of the hybrid channel will be affected when one of the component channels has an asymptotic outage probability that decays with SNR much faster than the other. In particular, we see that the overall SNR exponent will be dominated by the worst of the two component channel SNR exponents unless the binary code rate is below a certain threshold dependent on δ .

IV. ASYMPTOTIC OUTAGE ANALYSIS: CSIT CASE

Suppose both the transmitter and receiver have perfect knowledge of the CSI and the transmitter adapts the power to reduce the outage probability subject to constraints (3) and (4). The optimal power allocation strategy requires the solution to the following minimisation problem.

$$\begin{cases} \text{Minimise:} & \Pr \left\{ I_{\text{tot}}(\mathbf{p}, \hat{\mathbf{p}}, \mathbf{h}, \hat{\mathbf{h}}) < R \right\} \\ \text{Subject to:} & \mathbb{E}[\langle \mathbf{p} \rangle] + \mathbb{E}[\langle \hat{\mathbf{p}} \rangle] \leq P_{\text{av}}, \\ & \langle \mathbf{p} \rangle \leq P_{\text{peak}}^{\text{fso}}, \langle \hat{\mathbf{p}} \rangle \leq P_{\text{peak}}^{\text{rf}} \end{cases} \quad (17)$$

Theorem 4.1: The solution to problem (17) is given by

$$(\varphi^*, \hat{\varphi}^*) = \begin{cases} (\varphi, \hat{\varphi}) & \langle \varphi \rangle + \langle \hat{\varphi} \rangle \leq s^* \\ (\mathbf{0}, \mathbf{0}) & \text{otherwise,} \end{cases} \quad (18)$$

where $(\varphi, \hat{\varphi})$ is the solution to

$$\begin{cases} \text{minimise} & \langle \mathbf{p} \rangle + \langle \hat{\mathbf{p}} \rangle \\ \text{subject to} & I_{\text{tot}}(\mathbf{p}, \hat{\mathbf{p}}, \mathbf{h}, \hat{\mathbf{h}}) \geq R \\ & \langle \mathbf{p} \rangle \leq P_{\text{peak}}^{\text{fso}}, \langle \hat{\mathbf{p}} \rangle \leq P_{\text{peak}}^{\text{rf}} \\ & \mathbf{p}, \hat{\mathbf{p}} \geq \mathbf{0} \end{cases} \quad (19)$$

In (18), s^* is a threshold determined by $s^* = \sup \left\{ s : \mathbb{E}_{(\mathbf{h}, \hat{\mathbf{h}}) \in \mathcal{R}(s)} [\langle \varphi \rangle + \langle \hat{\varphi} \rangle] \leq P_{\text{av}} \right\}$, where $\mathcal{R}(s) \triangleq \left\{ (\mathbf{h}, \hat{\mathbf{h}}) \in \mathbb{R}^{A+B} : \langle \varphi \rangle + \langle \hat{\varphi} \rangle \leq s \right\}$.

Unfortunately, (19) is a non-convex optimisation problem [15], since in general $I_{\mathcal{X}}^{\text{awgn}}(p^2)$ is not a concave function in p . Thus (19). Instead of solving (19), we propose a suboptimal algorithm that, as we shall see, exhibits the same asymptotic behaviour as the optimal solution. In this direction, first consider the following lemmas. The proofs follow

straightforwardly via the Karush-Kahn-Tucker conditions [15] and using the relationship between mutual information and the minimum mean-square error (MMSE) for Gaussian channels [16].

Lemma 4.1: Define the minimisation problem,

$$\begin{cases} \text{minimise} & \langle \mathbf{p}^2 \rangle + \langle \hat{\mathbf{p}}^2 \rangle \\ \text{subject to} & I_{\text{tot}}(\mathbf{p}, \hat{\mathbf{p}}, \mathbf{h}, \hat{\mathbf{h}}) \geq R \\ & \mathbf{p}, \hat{\mathbf{p}} \succeq \mathbf{0}, \end{cases} \quad (20)$$

where $\langle \mathbf{p}^2 \rangle \triangleq \frac{1}{A} \sum_{a=1}^A p_a^2$. The solution to (20) is

$$p_a^* = \sqrt{\Upsilon_{\mathcal{X}_{\text{fso}}} \left(h_a^2 \rho^2, \frac{1}{n\lambda} \right)} \quad \text{and} \quad \hat{p}_b^* = \Psi_{\mathcal{X}_{\text{rf}}} \left(\hat{\rho} \hat{h}_b \gamma, \lambda \right), \quad (21)$$

where $\Upsilon_{\mathcal{X}}(u, t) \triangleq \frac{1}{u} \text{mmse}_{\mathcal{X}}^{-1}(\min\{\text{mmse}_{\mathcal{X}}(0), \frac{t}{u}\})$, $\Psi_{\mathcal{X}}(u, t)$ is the solution x to the equation $\text{mmse}_{\mathcal{X}}(xu) = \frac{2x}{tu}$, $\text{mmse}_{\mathcal{X}}(p)$ denotes the MMSE of a Gaussian channel with discrete input constellation \mathcal{X} , $\text{mmse}_{\mathcal{X}}^{-1}(u)$ is the inverse MMSE function, and λ is chosen such that $I_{\text{tot}}(\mathbf{p}, \hat{\mathbf{p}}, \mathbf{h}, \hat{\mathbf{h}}) = R$.

Lemma 4.2: Define the minimisation problem

$$\begin{cases} \text{minimise} & \langle \mathbf{p}^2 \rangle + \langle \hat{\mathbf{p}}^2 \rangle \\ \text{subject to} & I_{\text{tot}}(\mathbf{p}, \hat{\mathbf{p}}, \mathbf{h}, \hat{\mathbf{h}}) \geq R \\ & \sqrt{\langle \mathbf{p}^2 \rangle} \leq P_{\text{peak}}^{\text{fso}}, \sqrt{\langle \hat{\mathbf{p}}^2 \rangle} \leq P_{\text{peak}}^{\text{rf}} \\ & \mathbf{p}, \hat{\mathbf{p}} \succeq \mathbf{0} \end{cases} \quad (22)$$

Let \mathbf{p}^* and $\hat{\mathbf{p}}^*$ be the solution to (20) in Lemma 4.1, and \wp and $\hat{\wp}$ be the solution to (22). The solution to (22) is separated into four cases depending on \mathbf{p}^* and $\hat{\mathbf{p}}^*$.

1) If \mathbf{p}^* and $\hat{\mathbf{p}}^*$ satisfy the constraints in (22). Then $\wp = \mathbf{p}^*$ and $\hat{\wp} = \hat{\mathbf{p}}^*$.

2) If $\sqrt{\langle (\mathbf{p}^*)^2 \rangle} \leq P_{\text{peak}}^{\text{fso}}$ and $\sqrt{\langle (\hat{\mathbf{p}}^*)^2 \rangle} > P_{\text{peak}}^{\text{rf}}$. Then

$$\wp_a = \sqrt{\Upsilon_{\mathcal{X}_{\text{fso}}} \left(h_a^2 \rho^2, \frac{1}{n\lambda_1} \right)} \quad \text{and} \quad \hat{\wp}_b = \Psi_{\mathcal{X}_{\text{rf}}} \left(\hat{h}_b \gamma \hat{\rho}, \lambda_2 \right),$$

where λ_2 is chosen such that $\sqrt{\langle \hat{\wp}^2 \rangle} = P_{\text{peak}}^{\text{rf}}$ and λ_1 is chosen such that

$$\frac{n}{A} \sum_{a=1}^A I_{\mathcal{X}_{\text{fso}}}^{\text{awgn}}(\rho^2 h_a^2 \wp_a^2) = R - \frac{1}{B} \sum_{b=1}^B I_{\mathcal{X}_{\text{rf}}}^{\text{awgn}}(\hat{\wp}_b \hat{h}_b \hat{\rho} \gamma).$$

If $\sqrt{\langle \wp^2 \rangle} > P_{\text{peak}}^{\text{fso}}$ then the solution to (22) is infeasible.

3) If $\sqrt{\langle (\mathbf{p}^*)^2 \rangle} > P_{\text{peak}}^{\text{fso}}$ and $\sqrt{\langle (\hat{\mathbf{p}}^*)^2 \rangle} \leq P_{\text{peak}}^{\text{rf}}$. Then the solution to (22) is the same as the previous case, with the roles of rf and fso interchanged.

4) If $\sqrt{\langle (\mathbf{p}^*)^2 \rangle} > P_{\text{peak}}^{\text{fso}}$ and $\sqrt{\langle (\hat{\mathbf{p}}^*)^2 \rangle} > P_{\text{peak}}^{\text{rf}}$, then the solution to (22) is infeasible.

Comparing (19) with (22), we see that (22) is minimising the sum of the mean-square power of the FSO and RF channels, subject to individual short-term root mean-square (RMS) power constraints. By applying Jensen's inequality [11] to these constraints, we see that a solution to (22) will also satisfy the constraints in (19) and hence can be considered a suboptimal solution to (19). Therefore to find a suboptimal

solution to the original minimisation problem (17) we use the solutions in Lemma 4.2 for $(\wp, \hat{\wp})$ instead of solving (19).

The asymptotic outage performance of optimal power allocation for discrete-input block-fading AWGN channels was analysed by Nguyen *et al.* in [17], [18]. In particular, from [17, Prop. 3], if the peak-to-average power ratios α_{fso} and α_{rf} are finite, then the SNR exponent will be the same as the CSIR case given in Theorems 3.1 and 3.2. When there are no peak-to-average power constraints then the SNR exponent of the optimal power allocation strategy is [18, Th. 2]

$$d_{\text{csit}}^{(1)} = \begin{cases} \infty & d_{\text{csir}}^{(1)} > 1 \\ \frac{d_{\text{csir}}^{(1)}}{1-d_{\text{csir}}^{(1)}} & d_{\text{csir}}^{(1)} < 1, \end{cases} \quad (23)$$

where $d_{\text{csir}}^{(1)}$ is the SNR exponent for the CSIR case.

Theorem 4.2: Suppose $\alpha_{\text{fso}}, \alpha_{\text{rf}} \rightarrow \infty$. Then the SNR exponent of the suboptimal power allocation scheme described by (17) with (22) is given by (23).

The implications of (23) are described as follows. When $d_{\text{csit}}^{(1)} = \infty$, then the outage probability curve will be vertical at a certain threshold of average power, i.e. the hybrid system is able to maintain a constant level of instantaneous input-output mutual information. The threshold at which this occurs is referred to as the *delay-limited capacity* of the system [19]. Note that if $d_{\text{csir}}^{(1)} = 1$ in (23) then $d_{\text{csit}}^{(1)} = \infty$, however, the outage curve will not go vertical, nor will it converge to a constant slope when plotted on a log-log scale [17]. When the peak-to-average power ratios are finite, the peak power constraints introduce an error floor with a slope equal to the CSIR case. The height of the error floor is dependent on α_{fso} and α_{rf} [17].

To demonstrate the implications of our asymptotic results, we conducted a number of Monte Carlo simulations. Whilst our results cover a wide range of hybrid system parameters and fading distributions, due to space limitations, we will focus on one particular set of specifications, i.e.: an RF carrier employing 64QAM; an FSO carrier employing 4PPM; $A = B = 1$, $m + nq = 24$ bits, $\delta = \frac{3}{4}$; and exponential scintillation on both channels (modelling very strong turbulence). Fig. 1(a) shows the hybrid outage performance with our suboptimal power allocation strategy compared to uniform power allocation (cross marked curve) when $R_c = 1/4$. Note that $d_{\text{fso}}^{(1)} = d_{\text{rf}}^{(1)} = 1$. Thus, from Corollary 3.1, $d_{\text{csir}}^{(1)} = 2$, and from (23), the SNR exponent is $d_{\text{csit}}^{(1)} = \infty$, i.e. when there are no peak power constraints, the curve will go vertical at a certain average power threshold. This can be seen in Fig. 1(a) (thick solid curve), for $P_{\text{av}} > 7$ dB outages are completely removed. We see that there is a power saving of more than 20 dB compared to uniform power allocation to achieve 10^{-4} outage probability. When peak power constraints are introduced, as expected, we see that an error floor is introduced with the same slope as the CSIR case. The floor shifts down in probability as the peak-to-average power ratio increases. Fig. 1(b) shows the case when $R_c = 5/6$. Since $d_{\text{csir}}^{(1)} = 1$, when there are no peak power constraints, the

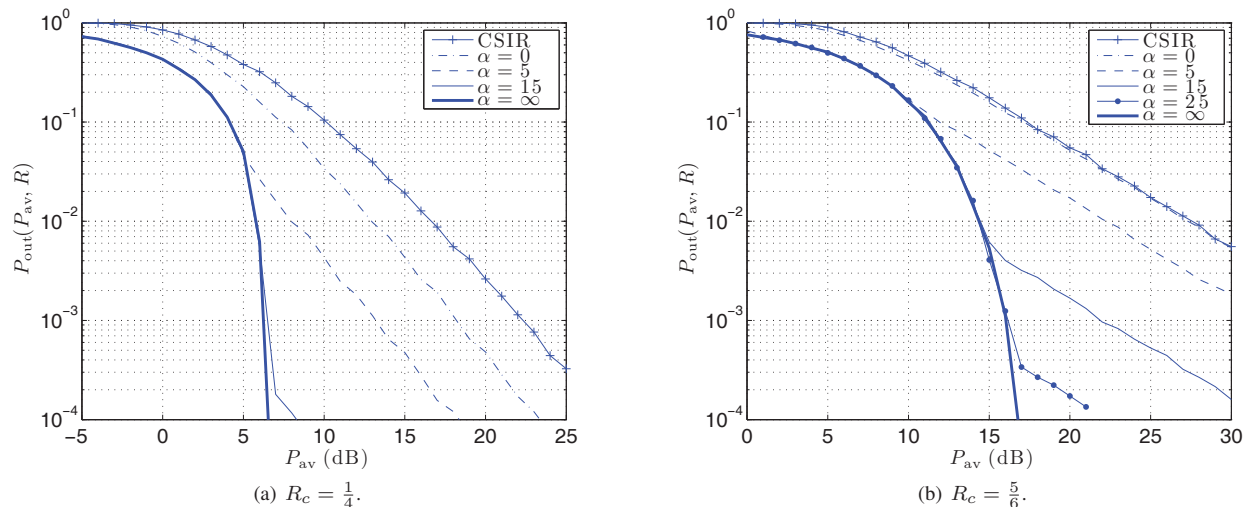


Fig. 1. Outage performance of the hybrid FSO/RF channel with CSIT (solid) and uniform power allocation (dashed). System parameters included: $\rho = \hat{\rho} = 0.5$, $A = B = 1$, $n = 9$, 4PPM FSO and 64QAM RF with peak and average power constraints, and peak-to-average power ratios $\alpha_{\text{fso}} = \alpha_{\text{rf}} = \alpha$ in decibels. Exponential distributed fading on both channels.

outage curve will no longer go vertical (thick solid curve). As expected we see an error floor is introduced when the peak-to-average power ratio is finite.

V. CONCLUSIONS

We proposed a simple hybrid FSO/RF channel model based on parallel block fading channels. This hybrid model takes into account differences in signalling rates and fading effects typically experienced by the component channels involved. Under this framework, we examined the information theoretic limits of the hybrid channel. In particular, we studied its asymptotic high SNR outage performance by analysing the outage diversity or SNR exponents. When CSI is only available at the receiver, in the general case, the exponent is not available in closed form. Instead, we derived simple expressions from which it can be computed numerically. When CSI is also available at the transmitter, we derived the optimal power allocation scheme that minimises the outage probability subject to peak and average power constraints. Due to the power scaling of the FSO channel, this requires the solution to a non-convex optimisation problem, which is intractable in practical systems. We proposed a suboptimal power allocation strategy, which is much simpler to implement and has the same SNR exponent as the optimal power allocation.

REFERENCES

- [1] L. C. Andrews and R. L. Phillips, *Laser Beam Propagation through Random Media*, SPIE Press, USA, 2nd edition, 2005.
- [2] N. Letzepis and A. Guillén i Fàbregas, "Outage probability of the Gaussian MIMO free-space optical channel with PPM," *IEEE Trans. Commun.*, vol. 57, no. 12, Dec. 2009.
- [3] S. M. Navidpour, M. Uysal, and M. Kavehrad, "BER performance of free-space optical transmission with spatial diversity," *IEEE Trans. Wireless Commun.*, vol. 6, no. 8, pp. 2813–2819, August 2007.
- [4] K. Chakraborty, S. Dey, and M. Franceschetti, "On outage capacity of MIMO Poisson fading channels," in *Proc. IEEE Int. Symp. Inform. Theory*, July 2007.
- [5] S. G. Wilson, M. Brandt-Pearce, Q. Cao, and J. H. Leveque, "Free-space optical MIMO transmission with Q -ary PPM," *IEEE Trans. Commun.*, vol. 53, no. 8, pp. 1402–1412, Aug. 2005.
- [6] F. Nadeem, B. Flecker, E. Leitgeb, M. S. Awan, and T. Javornik, "Comparing the fog effects on hybrid network using optical wireless and GHz links," in *Proc. Int. Symp. Commun. Sys., Networks and Digital Signal Proc.*, Jun. 2008, pp. 278–282.
- [7] T. Kamalakis, I. Neokosmidis, A. Tsiouras, S. Pantazis, and I. Andrikopoulos, "Hybrid free space optical / millimeter wave outdoor links for broadband wireless access networks," in *Proc. Int. Symp. Personal, Indoor and Mobile Radio Commun.*, Aug. 2007.
- [8] S. Vangala and H. Pishro-Nik, "A highly reliable FSO/RF communication system using efficient codes," in *Proc. IEEE Global Commun. Conf.*, 2007.
- [9] C. E. Mayer, B. E. Jaeger, R. K. Crane, and X. Wang, "Ka-band scintillations: measurements and model predictions," *Proc. IEEE*, vol. 85, no. 6, pp. 936–945, Jun. 1997.
- [10] M. S. Alouini, S. A. Borgsmiller, and P. G. Steffes, "Channel characterization and modeling for Ka-band very small aperture terminals," *Proc. IEEE*, vol. 85, no. 6, pp. 981–997, Jun. 1997.
- [11] T. M. Cover and J. A. Thomas, *Elements of Information Theory*, Wiley Series in Telecommunications, 1991.
- [12] N. Letzepis, K. D. Nguyen, A. Guillén i Fàbregas, and W. G. Cowley, "Hybrid free-space optical and radio-frequency wireless communication," *IEEE J. Select. Areas Commun. (special issue on optical wireless communications)*, vol. 27, no. 9, Dec. 2009.
- [13] S. Dolinar, D. Divsalar, J. Hamkins, and F. Pollara, "Capacity of pulse-position modulation (PPM) on Gaussian and Webb channels," *JPL TMO Progress Report 42-142*, Aug. 2000, URL: lasers.jpl.nasa.gov/PAPERS/OSA/142h.pdf.
- [14] R. M. Gagliardi and S. Karp, *Optical communications*, John Wiley & Sons, Inc., Canada, 1995.
- [15] S. Boyd and L. Vandenberghe, *Convex Optimization*, Cambridge University Press, 2004.
- [16] D. Guo, S. Shamai, and S. Verdú, "Mutual information and minimum mean-square error in Gaussian channels," *IEEE Trans. Inf. Theory*, vol. 51, no. 4, pp. 1261–1282, Apr. 2005.
- [17] K. D. Nguyen, A. Guillén i Fàbregas, and L. K. Rasmussen, "Power allocation for block-fading channels with arbitrary input constellations," *IEEE Trans. Wireless Commun.*, vol. 8, no. 5, pp. 2514–2523, May 2009.
- [18] K. D. Nguyen, A. Guillén i Fàbregas, and L. K. Rasmussen, "Outage exponents of block-fading channels with power allocation," *to appear IEEE Trans. Inf. Theory*, May 2010.
- [19] S. V. Hanly and D. N. C. Tse, "Multiaccess fading channels. II. delay-limited capacities," *IEEE Trans. Inf. Theory*, vol. 44, no. 7, pp. 2816–2831, Nov. 1998.